Fluorescent organic nanoparticle formation in lysosomes for cancer cell recognition†

Hsin-Hung Lin, Sheng-Yuan Su and Cheng-Chung Chang*

Received 5th February 2009, Accepted 27th March 2009
First published as an Advance Article on the web 7th April 2009
DOI: 10.1039/b902399b

We present a convenient method to prepare fluorophores 3- or 3,7-divinyl substituted 10*H*-phenothiazines and their protonation forms can aggregate to become fluorescent organic nanoparticles (FONs) with bright fluorescent spots in the lysosomes of cancer cells but not normal cells.

Cancer imaging using an optical technique is a sensitive, non-invasive, and relatively inexpensive technique that has strong potential for sensitive cancer diagnosis. In recent years, fluorescent organic nanoparticles (FONs) have received considerable attention.[1,2] Different from quantum dots and polymer nanoparticles, FONs are expected to play various roles in a wide variety of applications such as optoelectronic devices due to the flexibility of synthetic approaches to such organic small compounds.[2] The switching of emission properties of FONs is often size-dependent and related to the effects of intramolecular planarization or specific intermolecular aggregation conformation. However, there are not many relevant topics on the application of FONs for cellular diagnosis. The phenothiazine (PTZ) core has been considered to be an important moiety in heterocyclic chemistry after it was first reported in 1883.[3] The well-defined electron-donating properties[4] of PTZ can be partially associated with electrophores as it was widely used in organic light-emitting diodes (OLEDs),[5] acid–base dyes and pigments,[6] near-IR dyes,[7] semiconductors,[4,8] or chemical sensors[9] in material science.

Department of Chemistry, National Chung Hsing University, 250, Kuo Kuang Road, Taichung, 402, Taiwan, R.O.C. E-mail: ccchang555@dragon.nchu.edu.tw; Fax: +886-4-22862547

† Electronic supplementary information (ESI) available: Experimental materials, spectra and quantum yields measurements, cell culture incubation, confocal cellular localizations, protonation spectra and solvent effect. See DOI: 10.1039/b902399b

In this manuscript, we present a convenient method to prepare 3- or 3,7-divinyl substituted 10*H*-phenothiazines (PVP and BPVP) and build a donor–acceptor model as shown in Scheme 1. The basicities of PVP and BPVP are evaluated since both fluorophores can be partially protonated by lysosomes in the cells; the protonated molecules, $PVPH^+$ and $BPVPH^+$, can then aggregate to form fluorescent organic nanoparticles (FONs) with bright fluorescent spots, which are clearly observed under a confocal microscope. We developed optimized conditions for the aggregation-induced enhanced emission (AIEE) properties of these PTZ derivatives, and their related nanoparticles were observed by transmission electron microscopy (TEM) images *in vitro*. Most importantly, the bright fluorescent spots in lysosomes of cancer cells, which were formed from the FONs, can be used in recognizing cancer cells due to their multiple fluorescence characteristics.

The basic spectra of these compounds in DMSO solutions are provided in Fig. 1. PVP and BPVP present well-defined extinction coefficients and quantum yields in the visible region. Once protonation is completed, the absorption bands of PVP and BPVP show bathochromic shifts and the intensities of emission peaks decrease in their quantum yields but with no apparent peak shifts. We suggest that electron transfer from the phenothiazine donor to the pyridinium acceptor and, subsequently, ground state intramolecular charge transfer (ICT) is enhanced.[10] However, the excited state photo-induced electron transfer (PET) is weakened.[11] Since the intensities of emissions are almost quenched in excess acid, protonation spectra in Fig. 1 are presented with the end points of protonation titration curves (Figure S1) of PVP and BPVP in DMSO solutions. In order to estimate pK_a values, spectral changes as a function of pH for compounds PVP and BPVP were measured in DMSO/H_2O (5/95, v/v) solutions, and their titration fitting curves are shown in Fig. 2. The pK_a values (also listed in Scheme 1) for the first protonation of

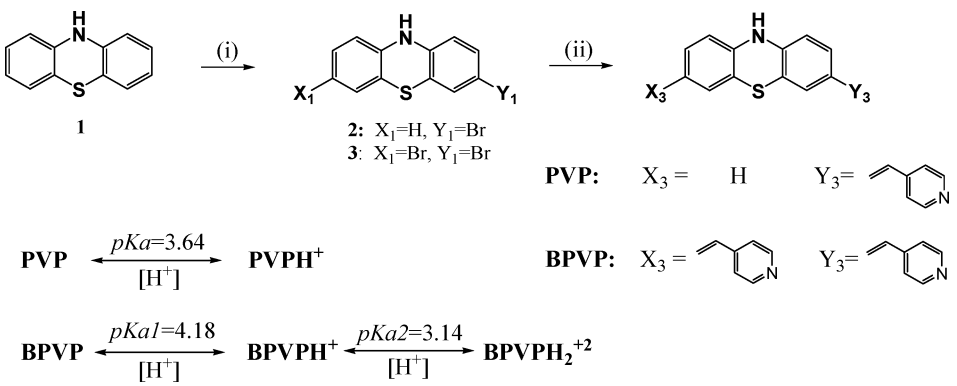

Scheme 1 Synthesis and protonation illustrations of PVP and BPVP. *Reaction reagents and conditions*: (i) NBS/THF, rt, 6 h; (ii) $Pd(OAc)_2$/(o-tol)$_3$P, 4-vinylpyridine, Et_3N/MeCN, N_2, 48 h.

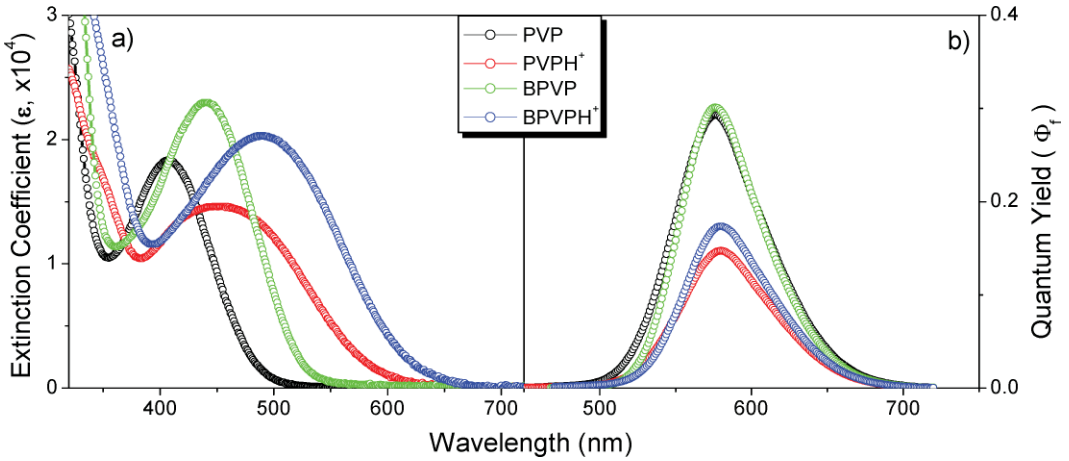

Fig. 1 (a) Absorption and (b) emission spectra for neutral and protonated PVP and BPVP in DMSO solutions. ε: extinction coefficients (M^{-1} cm^{-1}), Φ: quantum yields (using Rhodamine Green as a standard). Protonation spectra were measured from the end points of the protonation titration curves of PVP and BPVP in DMSO solutions, respectively.

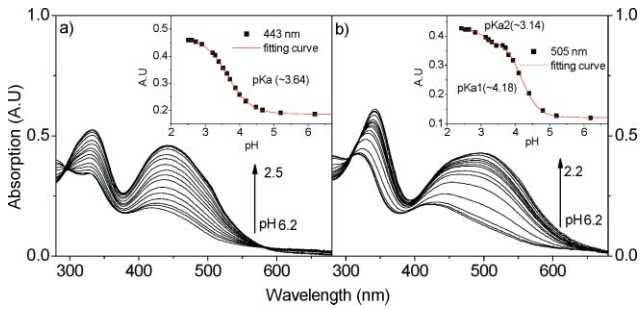

Fig. 2 Absorption spectra of 25 μM (a) PVP and (b) BPVP in DMSO/H_2O (5/95, v/v) as a function of pH. The insets show the absorption intensity plots (443 nm for PVP, 505 nm for BPVP) and their pK_a fitting curves (pK_a values are shown as Scheme 1).

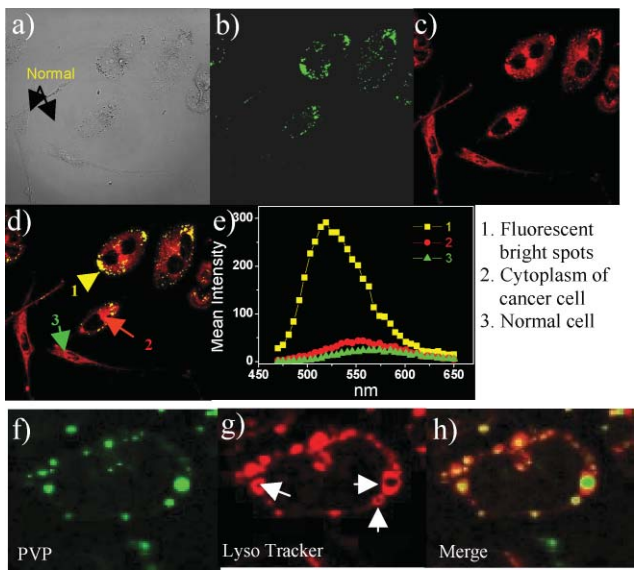

Fig. 3 Confocal microscopy images of co-cultured CL1-0 lung cancer and MRC-5 normal lung fibroblast cell lines. Cells were incubated with 6 μM BPVP for 4 h, and a 405 nm diode laser was used as the light source. (a) Bright field image; (b) spectra recorded at 420–530 nm in PMT 1; (c) 530–650 nm in PMT 2; (d) merger of (b) with (c); (e) λ scan from 470 to 650 nm with 5 nm integration. The spectra were obtained from the average of 50 individual cancer and normal cells. (f)–(h): Magnified images of 4 μM PVP co-staining with LysoTracker in a CL1-0 lung cancer cell. The excitation source was a 405 nm diode laser for PVP compounds and a 561 nm DPSS green laser for markers. Fluorescence photographs were taken through related 420–530 nm (f) and 580–700 nm (g) ranges.

the compounds PVP (pK_a ~ 3.64) and BPVP (pK_a ~ 4.18) are lower with respect to pyridine (~5.2), 2-vinyl pyridine (~4.8), and the fluorescent pH indicator Oregon Green® 488 (~4.7)[12]; while, in accord with distyryl-pyridine derivatives.[13] The expected stabilization of the protonated species ($PVPH^+$ and $BPVPH^+$) show a lower pK_a, indicating that a resonance effect between PTZ and pyridine moieties decreases the basicity of the first protonation site. Obviously, further protonation at another pyridine ring of BPVP occurs at pK_a ~ 3.14 as compared to PVP. Furthermore, excess acids can lead to the protonation of the 10 position N atom on the PTZ moiety of PVP (pK_a ~ 0.71) and BPVP (pK_a ~ 0.22). However, we have not provided a more detailed discussion as this acidic process is not involved in the application of cellular staining.

The cellular staining results of compounds PVP and BPVP in co-cultured MRC-5 normal lung fibroblast cells and CL1-0 lung cancer cells are noteworthy. In contrast with the results observed in normal cells, cancer cells show bright spots by confocal microscopy (Fig. 3a–d) and the λ scanning spectra suggests a different emission wavelength of BPVP between normal and cancer cell lines (Fig. 3e). Similar results are also reproduced in other cancer cell lines (human osteosarcoma MG63, human lung adenocarcinoma cell line A549 and a transformed murine fibroblast L929 cancer line). Hence, we examined the immunofluorescence staining for the intracellular localization of PVP and BPVP using commercially available organelle probes (Figure S2). CL1-0 cancer cells were incubated first with a compound for 4 h and then with the organelle probes (MitoTracker Red CM-H2XRos for 30 min at 37 °C; LysoTracker Red DND-99 for 30 min at 37 °C). The fluorescent bright spots were observed to colocalize with the lysosomal markers, and the residues barely colocalized with the mitochondrial markers. These results indicate that PVP and BPVP molecules generally spread in the cytoplasm of living cells and accumulate in lysosomes to result in the bright spots. The bright

spots of lysosomes from PVP and BPVP both show stronger emission bands at ~515 nm than residual remains in the cytoplasm (560~580 nm), which is very similar to the emission peak positions of free or protonated compounds in bulk solutions. Similar λ scanning spectra between PVP and BPVP are observed as expected since their emission spectra centers and intensities are also similar either in aqueous or DMSO solutions. Owing to these distinct cellular staining patterns, we believe that both PVP and BPVP can be used to differentiate cancer cells from normal cells once suitable filters (510–530 nm) are constructed The image is shown in Fig. 3b in which only cancer cells brighten up in the cell staining image.

In fact, after carefully examining the immunostaining images, we observed that the bright spots do not fully merge with LysoTracker but stay inside the lysosomal membrane (Fig. 3f–h). Based on our knowledge, the enzymes contained in lysosomes act optimally at a low pH; thus, lysosomes maintain a low pH (~4.8) *via* proton-pumping vacuolar ATPases.[14] According to our pK_a studies, the pyridine moieties of compounds PVP and BPVP should be easily protonated or partially protonated in lysosomes, like the fluorescent pH indicator Oregon Green® 488, to become PVPH$^+$ and BPVPH$^+$. Then, the intensities of emissions should be quenched with peak locations remaining unchanged (as shown in Fig. 1). Therefore, the simple aggregation or solvent effect does not seem effective in fully explaining the dramatic increase in fluorescence in lysosomes of cancer cells. Thus, to elucidate the formation of bright spots, we studied the emission spectra of compounds PVP and BPVP under volume mixing ratios of solutions containing certain pH acidic aqueous solutions (pH = 3.95 for PVP, 4.21 for BPVP) and tetrahydrofuran (THF). Figs. 4a and 4b show a drastic change in the fluorescence intensity of PVP and BPVP in mixtures of acidic solution/THF.[15] The AIEE[16] properties reach maximum quantum yields in 25% volume

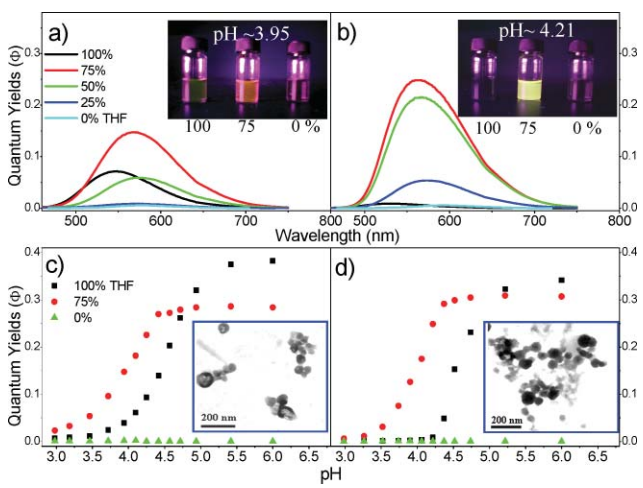

Fig. 4 Illustrations of FONs for PVP (a, c) and BPVP (b, d). Emission spectral variations under different mixing ratios of acidic aqueous solutions at pH ~ 3.95 for (a) PVP and ~4.21 for (b) BPVP in THF. Insets show the photographs obtained with the corresponding mixed solutions. (c) The intensity plots of emissions of 0, 25 and 100% of H_3O^+/THF mixed solutions containing PVP and (d) BPVP as functions of pH values, respectively. Insets show the TEM images of nanoparticles obtained with the corresponding mixed solution acidic solution/THF = 25/75 v/v (as inset images of (a) and (b)). Excitation wavelength for each solution is 400 nm for PV and 440 nm for BPVP.

fractions of the acidic water (as the insets in Fig. 4a and 4b) and their relative TEM images (insets of Figs. 4c and Figs. 4d) clearly show that PVPH$^+$ and BPVPH$^+$ nanoparticles are very fine spheres with a mean diameter of 50–100 nm. Based on previous studies,[2,3] it is known that the self-assembly of acidic PTZ compounds leading to the formation of spherical nanoparticles is accompanied by dramatic fluorescence changes. Alternatively, in the neutral water/THF mixed solutions, PVP and BPVP do not exhibit AIEE under the same experimental conditions. Thus, we conclude a FONs model in which FONs were formed with aggregations of PVPH$^+$ or BPVPH$^+$, but not PVP and BPVP, inside the vacuole of lysosomes of cancer cells. That is, even though we incubated cell lines with the neutral PVP or BPVP, the diversity of cellular images comes from the outstanding behavior of PVPH$^+$ or BPVPH$^+$.

We also investigated the FON formation conditions of PTZ derivatives under variable pH values and concentrations of compounds in solutions. The nanoparticles are easily observed in TEM images with varying concentrations from 5 to 100 μM in acidic aqueous/THF mixed solutions. In addition, the distinct AIEE are reproducible under the appropriate pH range (Figs. 4c and Figs. 4d). Thus, we evaluate the AIEE areas for PVPH$^+$ and BPVPH$^+$ with their demarcation between pH values of 3.2–4.7 and 3.5–5.2, respectively. When considering the dissociation ability of HCl in the THF solvent, the actual pH values of these mixed solutions should be higher than those marked in Fig. 4. Thus, AIEE areas in Figs. 4c and Figs. 4d should cover the acidic condition of lysosomes of living cells. On the other hand, either in organic or aqueous solutions, the fluorescent intensities of PTZ derivatives are decayed in the course of protonation. In addition, the spectral properties of BPVPH$_2^{+2}$ are very close to BPVPH$^+$, and the first protonation of BPVP is indistinguishable for the di-substituted pyridine. Consequently, we observe that the AIEE area of BPVPH$^+$ is wider than PVPH$^+$. In all, we suggest that the protonated species PVPH$^+$ or BPVPH$^+$ serve as surfactant-like molecules, which will further self-assemble to form micelle-like nanoparticles due to their amphiphilic characteristics (their critical micelle concentrations, CMC values, were determined in Figure S3). Thus, it is reasonable to build a FON model based on our studies, especially in the case of water/aprotic solvent mixed solutions. However, at present, we have no evidence to elucidate whether BPVPH$_2^{+2}$ produced in the cell or BPVPH$_2^{+2}$ can form FONs. Nevertheless, we evaluate the AIEE formation conditions and build a FON model for our PTZ derivatives. On the other hand, based on our confocal studies, we believe that neutral PTZ derivatives can locate in the lysosmes of cancer and normal cells, while only protonated PTZ derivatives which stay in the lysosome of cancer cells can form FONs and show the bright spot images. According to the discussion above, the pH difference of lysosomes between cancer and normal cells should be one of reasons to achieve the cellular image difference between cancer and normal cells.

Finally, we also explore the peak location of the λ scanning spectra in Fig. 3e. The solvent effect of PVPH$^+$ and BPVPH$^+$ instead of neutral compounds PVP and BPVP were measured as shown in Figure S4. Both the emission bands showed hypsochromic shifts along with hyperchromism in less polar solvents, especially in toluene, ethyl acetate, and THF. Notably, these spectra are collected under the first end point of the protonation titration process in every solvent. They suggest that PVP or BPVP penetrate

into the cell and are then protonated in lysosomes. Eventually, acidic compounds $PVPH^+$ or $BPVPH^+$ aggregate in the less polar vacuoles to form FONs (Figs. 3f–h). This finding confirms the AIEE results shown in Fig. 4—FONs are formed under the acidic solution/THF (75/25, v/v) condition but not THF/acidic solution (80/20, v/v) as described in literature.[2b,2d] Nevertheless, we conclude that fluorescence is enhanced when compounds stay in lysosomes but decreases in the cytoplasm. Further, these two compounds can be used as cancer cell recognizers due to their significant contrast in emission between cancer cells and normal cells.

In summary, this manuscript describes the synthesis and evaluation of a set of 10*H*-phenothiazine derivatives that have been modified in the 3 or 3,7- positions with electron-deficient pyridine groups *via* ethenyl linkers. Their AIEE properties were observed for both *in vitro* spectral studies and cellular staining. Finally, we developed a vacuole model using FONs to elucidate the formation of fluorescent bright spots, which are considered to form in the lysosomes of cancer cells. With appropriate tuning of the spectral characteristics of these compounds with regard to cellular staining, they can be used as biomarkers in cell biology.

Acknowledgements

This work was supported financially by the National Science Council (NSC 97-2113-M-005-001) of Taiwan. Thanks Ta-Chau Chang (Academia Sinica) for supporting cell lines and a number of helpful discussions.

Notes and references

1 H. S. Nalwa, H. Kasai, S. Okada, H. Oikawa, H. Matsuda, A. Kakuta, A. Mukoh and H. Nakanishi, *Adv. Mater.*, 1993, **5**, 758; H. Kasai, H. Kamatani, Y. Yoshikawa, S. Okada, H. Oikawa, A. Watanabe, O. Itoh and H. Nakanishi, *Chem. Lett.*, 1997, **26**, 1181; H. B. Fu and J. N. Yao, *J. Am. Chem. Soc.*, 2001, **123**, 1434; B. K. An, S. K. Kwon and S. Y. Park, *Angew. Chem., Int. Ed.*, 2007, **46**, 1978.
2 J. Luo, Z. Xie, J. Y. Lam, L. Cheng, H. Chen, C. Qiu, H. S. Kwok, X. Zhan, Y. Liu, D. Zhu and B. Z. Tang, *Chem. Commun.*, 2001, 1740; B. K. An, S. K. Kwon, S. D. Jung and S. Y. Park, *J. Am. Chem. Soc.*, 2002, **124**, 14410; D. Xiao, L. Xi, W. Yang, H. Fu, Z. Shuai, Y. Fang and J. Yao, *J. Am. Chem. Soc.*, 2003, **125**, 6740; Y. Y. Sun, J. H. Liao, J. M. Fang, P. T. Chou, C. H. Shen, C. W. Hsu and L. C. Chen, *Org. Lett.*, 2006, **8**, 3713; S. S. Palayangoda, X. Cai, R. M. Adhikari and D. C. Neckers, *Org. Lett.*, 2008, **10**, 281.
3 A. Bernthsen and B. Dent, *Chem. Ges.*, 1883, **16**, 2996.
4 B. N. Achar and M. A. Ashok, *Mater. Chem. Phys.*, 2008, **108**, 8.
5 G. W. Kim, M. J. Cho, Y. J. Yu, Z. H. Kim, J. I. Jin, D. Y. Kim and D. H. Choi, *Chem. Mater.*, 2007, **19**, 42; L. Yang, J. K. Feng and A. M. Ren, *J. Org. Chem.*, 2005, **70**, 5987.
6 C. O. Okafor, *Dyes Pigm.*, 1986, **7**, 249; J. J. Aaron, M. Maafi, C. Kersebet, C. Parkanyi, M. S. Antonious and N. Motohashi, *J. Photochem. Photobiol., A*, 1996, **101**, 127.
7 T. Okamoto, M. Kuratsu, M. Kozaki, K. Hirotsu, A. Ichimura, T. Matsushita and K. Okada, *Org. Lett.*, 2004, **6**, 3493.
8 S. Aftergut and G. P. Brown, *Nature*, 1962, **193**, 361.
9 M. Hauck, J. Schonhaber, A. J. Zucchero, K. I. Hardcastle, T. J. Muller and U. F. Bunz, *J. Org. Chem.*, 2007, **72**, 6714.
10 K. Rurack, M. Kollmannsberger and J. Daub, *Angew. Chem., Int. Ed.*, 2001, **40**, 385; X. Peng, F. Song, E. Lu, Y. Wang, W. Zhou, J. Fa and Y. Gao, *J. Am. Chem. Soc.*, 2005, **127**, 4170.
11 A. P. Silva, H. N. Gunaratne, T. Gunnlaugsson, A. M. Huxley, C. P. McCoy, J. T. Rademacher and T. E. Rice, *Chem. Rev.*, 1997, **97**, 1515; H. Sunahara, Y. Urano, H. Kojima and T. Nagano, *J. Am. Chem. Soc.*, 2007, **129**, 5597.
12 P. M. Haggie and A. S. Verkman, *J. Biol. Chem.*, 2007, **282**, 31422.
13 A. Bailistreri, L. Gregoli, G. Musumarra and A. Spalletti, *Tetrahedron*, 1998, **54**, 9721.
14 I. Kazuhiro, A. Takafumi and G. Hidemi, *BioTechniques*, 2008, **45**, 465.
15 Preparation of mixed solutions: we directly mix THF with certain pH dd water. While the acidic THF solution (as we assign 0% acidic aqueous water) is achieved by adding an equal concentration of HCl (volume < 5%) to make the aqueous solution become pH = 4.21 or 3.95, as shown in Fig. 4.
16 B. K. An, D. S. Lee, J. S. Lee, Y. S. Park, H. S. Song and S. Y. Park, *J. Am. Chem. Soc.*, 2004, **126**, 10232.